Optica Applicata, Vol. LIII, No. 4, 2023
DOI: 10.37190/oa230406

Creation of vector Bessel beams with arbitrary polarization modes using mode extraction principle

Lingyu Wang, Xiaojie Sun, Guanxue Wang, Xiangyu Kang,
Ziyan Li, Xiumin Gao*, Songlin Zhuang

University of Shanghai for Science and Technology, Shanghai 200093, China

*Corresponding author: gxm@usst.edu.cn

According to the current research on polarization generation methods, it is difficult to create multi-mode vector Bessel beams in free space by extracting arbitrary polarization modes from a single beam. This is due to the fact that the polarization and phase distributions between multiple polarization modes can interfere with each other. In this paper, the mode extraction principle is combined with the optical pen technique to extract arbitrary polarization modes from a single Bessel beam, and the number, position and phase of Bessel beams can be arbitrarily regulated to achieve the multi-mode coexistence of vector Bessel beams in free space. The experimental results are consistent with the theoretical analysis. This work is not only important for the in-depth study of vector Bessel beams, but also will facilitate the development of optical manipulation, optical communication, microscopic imaging and other applications.

Keywords: vector Bessel beam, the mode extraction principle, arbitrary polarization modes.

1. Introduction

Bessel beam is a special diffraction-free beam satisfying the Helmholtz wave equation [1] and has a longer transmission distance than Gaussian-like beam [2]. Therefore, it is widely used in high-resolution imaging [3,4], laser processing [5-7], particle manipulation [8-11], optical communication [12-14] and other fields. Orthogonal electric field vector composed of linear and circular polarization can be utilized to construct arbitrary polarization distributions, such as radial and angular polarization, which satisfy the Helmholtz wave equation. Bessel beams constructed based on vector beams have more significant advantages over linearly polarized Bessel beams. For example, the imaging contrast can be significantly improved [15], background noise can be reduced [16], and the stability performance and transmission rate of communication [17,18] can be improved. Therefore, the research of vector Bessel beams has become a hot topic.

The free-space communication capacity based on orbital angular momentum multiplexing can be increased by a factor of two if vector polarized modes are em-

ployed [19,20]. By focusing the vector beam, the diffraction limit can be exceeded; however, that is considered to be impossible in the framework of scalar optics [21]. Vector polarization optimization has become a core technology for improving optical resolution [22]. All these illustrate that the modulation of the vector polarization mode plays an extremely important role in many optical fields. In addition, a vector beam that can freely adjust the degree of polarization and spatial freedom can provide more available states. For example, the manipulation degree of freedom for particle trapping can be increased [23], and the resolution of optical imaging can be improved [24]. The space-variant polarization states of vector Bessel beam can induce the vectorial Doppler effect as well [25]. They also have use in quantum entanglement [26] and quantum regime for metrology [27] due to their intriguing properties.

Vector Bessel beams generation methods and arbitrary polarization generation are extensively explored by scientists. Axicon [28] and quantized Pancharatnam–Berry (PB) phase optical elements [29] are adopted to generate vector Bessel beams, and the PB device introduces the spatially varying phase distribution by adjusting the direction of the spatially varying half-wave plate. Arbitrary polarization states will be generated through polarization selective devices [30]. At the same time, interference technology [31] is also employed to combine two orthogonal polarization modes to generate different polarization distributions. However, these methods can only generate a vector Bessel beam with relatively single polarization modes and cannot dynamically adjust the number, position, and amplitude of vector Bessel beams to form an array of vector Bessel beams due to the lack of flexibility. This will limit some applications of vector Bessel beams. Therefore, Huygens sub-metasurface has been used to generate high-efficiency and ultra-compact Bessel beam arrays [32], while the generation of vector Bessel beams with multiple polarization modes has not been investigated in detail. This stems from that the complex polarization structure and phase structure of a single beam are entangled with each other under the multi-mode coexistence condition. Consequently, it is quite hard to extract arbitrary polarization state from a single beam. A method to break this inherent polarization mode is urgently needed to extract arbitrary polarization mode from vector Bessel beams, thus facilitating the development of multi-dimensional manipulation of light field.

Combining previous studies on the principle of mode extraction [33] and the optical pen technique [34], this study proves the possibility of extracting arbitrary polarization modes from a single beam to create a vector Bessel beam with multi-mode coexistence. The experimental results are compatible with the theoretical analysis. The axicon phase, vortex phase and phase of polarization mode are introduced. Here, the mode extraction technique is the inverse process of interference technique. The optical pen is able to arbitrarily regulate the number, position, and phase of vector Bessel beams to generate vector Bessel beam arrays. In combination with mode extraction technology, the multi-mode extraction of Bessel beams in free space is achieved. In current study, the extraction of the arbitrary polarization mode of vector Bessel beams in free space will provide new ideas for the development of the light field and related applications.

2. Theory

The focusing system for arbitrary polarization mode extraction of Bessel beams is shown in Fig. 1. The focusing system is depicted in Fig. 1(a), where P is the pupil filter. The phase of the vector Bessel beam is described in Fig. 1(b). The phase of the scalar Bessel beam is firstly generated by combining the vortex phase with the axicon phase. The phase of the scalar Bessel beam is then combined with the polarization to generate the phase of the vector Bessel beam. Figure 1(c) is extracted by modulating phase (b). The polarization mode of the Bessel beam after extracting the focusing region of the mirror from a collimated incident $m = 30$-order vector vortex beam (VVB) is propagating in the proper phase along the optical axis. Here, the phase is placed at the pupil filter of objective lens (OL). As demonstrated in our previous works, the number, position and amplitude, phase of multiple VVBs can be adjusted at will by the optical pen, while their orders are manipulated based on the principle of mode extraction [33,34]. Here, the principle of mode extraction represents an inverse process of interferometric techniques that enables to extract arbitrary desired polarization mode from a single light beam, namely high order vector Bessel beam in our paper. This work presents an example on how to create the polarization mode of an arbitrary Bessel beam using the principle of mode extraction, which may offer new opportunities for the applications of the vector Bessel beam.

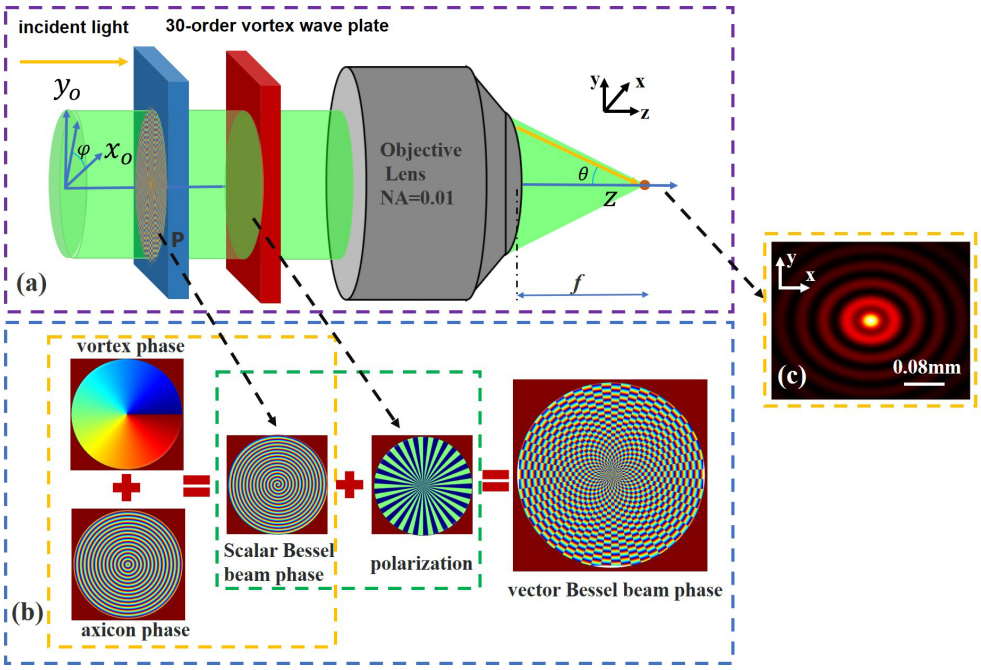

Fig. 1. Schematic diagram of focusing system for arbitrary polarization mode extraction of Bessel beams. (a) Focusing system, where P is the pupil filter. (b) The phase of the vector Bessel beam. (c) The intensity distribution extracted by the modulation phase (b).

According to the vector Debye diffraction theory, the electric field can be expressed as [35]

$$\mathbf{E} = \frac{-iA}{\pi}\int_0^{\alpha}\int_0^{2\pi}\sqrt{\cos\theta}\,\sin\theta\,\mathbf{V}\,l_0(\theta)T\exp(-ik\mathbf{s}\cdot\boldsymbol{\rho})\mathrm{d}\varphi\mathrm{d}\theta \tag{1}$$

where θ and φ respectively are the convergence and azimuth angles, A denotes a normalization constant. $\alpha = \arcsin(\mathrm{NA}/v)$, where NA is the numerical aperture of the objective, v ($v = 1$) represents the refractive index of the focusing space. The wave number $k = 2\pi v/\lambda$, in which λ represents the wavelength of the incident beam. $\boldsymbol{\rho} = (r\cos\varphi, r\sin\varphi, z)$ is the position vector of any observation point in the focusing field. $\mathbf{s} = (-\sin\theta\cos\varphi, -\sin\theta\sin\varphi, \cos\theta)$ denotes the unit vector in the polar coordinate system along the direction of the convergence ray. $T = \exp(i\psi)$ is the transmittance function of the optical pupil filter, and ψ indicates the phase distribution of the optical pupil filter. $l_0(\theta)$ represents the electric amplitude of the incident Gaussian beam [36], which can be expressed as

$$l_0(\theta) = \exp\left[-\left(\beta_0\frac{\sin\theta}{\sin\alpha}\right)^2\right] \tag{2}$$

where β_0 is the ratio of the pupil radius to the incident beam waist.

$\mathbf{V}$ represents the unit vector of propagation of the incident beam right after having passed through the lens. Therefore, $\mathbf{V}$ can be written as [37,38]

$$\mathbf{V} = \cos(m\varphi)\mathbf{V}_x + \sin(m\varphi)\mathbf{V}_y \tag{3}$$

where, $\mathbf{V}_x$ and $\mathbf{V}_y$ denote the electrical vectors of $|x\rangle$ and $|y\rangle$, where and denote the x and y linear polarization modes, respectively. $\mathbf{V}_x$ and $\mathbf{V}_y$ can be expressed as

$$\mathbf{V}_x = \begin{bmatrix}\sin^2\varphi(1-\cos\theta)+\cos\theta\\ \cos\varphi\sin\varphi(\cos\theta-1)\\ \cos\varphi\sin\theta\end{bmatrix}, \quad \mathbf{V}_y = \begin{bmatrix}-(1-\cos\theta)\sin\varphi\cos\varphi\\ 1-(1-\cos\theta)\sin^2\varphi\\ \sin\varphi\sin\theta\end{bmatrix} \tag{4}$$

The generation of the vector Bessel beam relies on the modulation term T_j. Here, the axicon phase is $T_\alpha = \exp(-i\cdot 2\pi r/d)$, where d is the period of axicon, $r = \sin\theta/\mathrm{NA}$. The vortex phase $T_1 = \exp(il\varphi)$, where l denotes topological number.

The vector Bessel beam has a complex spatial polarization pattern. To identify the polarization pattern of the generated vector Bessel beam, we use a pattern extraction method. The m-order vector beam is modulated by adding a polarization mode phase T_p, together with the vortex phase T_l and the axicon phase T_a. Here, the polarization mode phase T_p can be written as

$$T_\mathrm{p} = \mathrm{phase}(\cos(q\varphi+\beta)) \tag{5}$$

where β represents the polarization direction, and $q = m - n$, while m represents the order of the vortex plate, where $m = 30$.

Thus the modulation symmetry of the polarization is broken, the target mode is separated from the others, and then only the desired target mode is retained by filtering. Finally, the obtained modulation term T_j can be expressed as

$$T_j = \exp\left(-i\frac{2\pi r}{d}\right)\exp(il\varphi)T_{\mathrm{p}} \tag{6}$$

According to the previous research of the optical pen, it is combined with T_j. Therefore, the transmittance function of the optical pupil filter T in Eq. (1) can be expressed as

$$T = T_j \exp\left[i\sum_{j=1}^{N}\mathrm{PF}(s_j, x_j, y_j, z_j, \delta_j)\right] \tag{7}$$

where $\mathrm{PF}(x_j, y_j, z_j)$ is the optical pen, which was derived using the optical path compensation. N is the number of foci and j denotes the j-th focus. x_j, y_j, and z_j are the position coordinates of the j-th focal point on the focal sphere. δ_j represents the weighting factor used to adjust the phase of the j-th focal point, and s_j is utilized to adjust the amplitude of the j-th focal point [35].

3. Simulation results and discussion

In the following simulations, NA = 0.01. The unit of length in all figures is the wavelength λ, and the light intensity is normalized to a unit value.

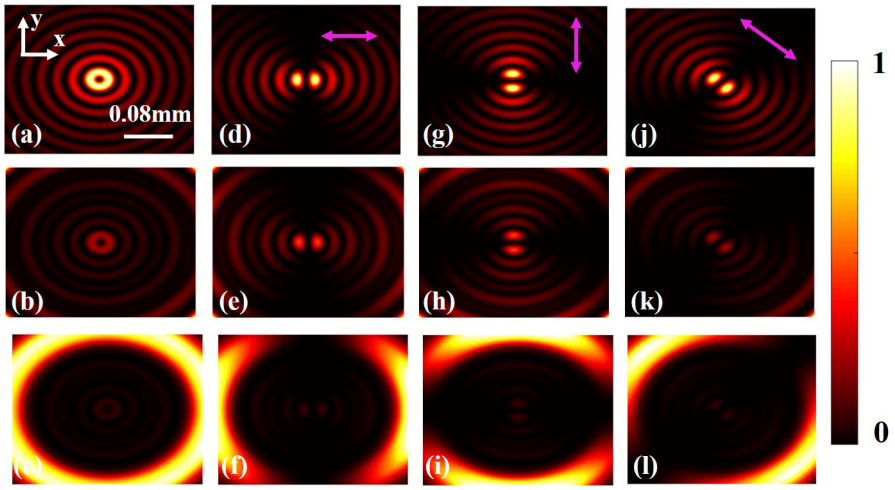

Fig. 2. Focusing field distribution of Bessel beam with different parameters d. The parameters d are 0.07 (first row), 0.2 (second row), and 0.3 (third row), where $\beta = 0$, $l = 0$, $n = 1$. (a)–(c) are total field. Subfigures ((d)–(f), (g)–(i), (j)–(l)) show the light intensities passing through the polarizer indicated by the pinkish purple arrows. The light intensities are normalized to a unit value.

According to the theoretical model, the generation of Bessel beams can be influenced by the period d of the transmission function of the axicon. In order to study the extraction of different polarization modes of a vector Bessel beam better, we firstly determine the parameter d. It is calculated by the equation $d = \lambda f / r_0$, where λ is wavelength, f is focal length, and r_0 is the radius of the aperture in the focusing system [39]. We choose $d = 0.07, 0.2, 0.3$ to observe the focusing field distribution, as shown in Fig. 2.

Figure 2 shows the influence of different periods of axicon d on the Bessel beam. We set $n = 1$, $l = 0$, $\beta = 0$. It can be seen that the profile of the Bessel beam is no longer maintained with the d increasing. Especially, the Bessel beam has the best profile at $d = 0.07$. Here, $d = 0.07$ is chosen as the best parameter.

In this section, we focus on analyzing the polarization mode extraction results of vector Bessel beams with different topological numbers $l = 0$, 1, 2, as respectively shown in Figs. 3–5. Here, we set the polarization direction $\beta = 0$, the period of axicon $d = 0.07$. The orientations of the polarizer are 0°,90°, and 135°.

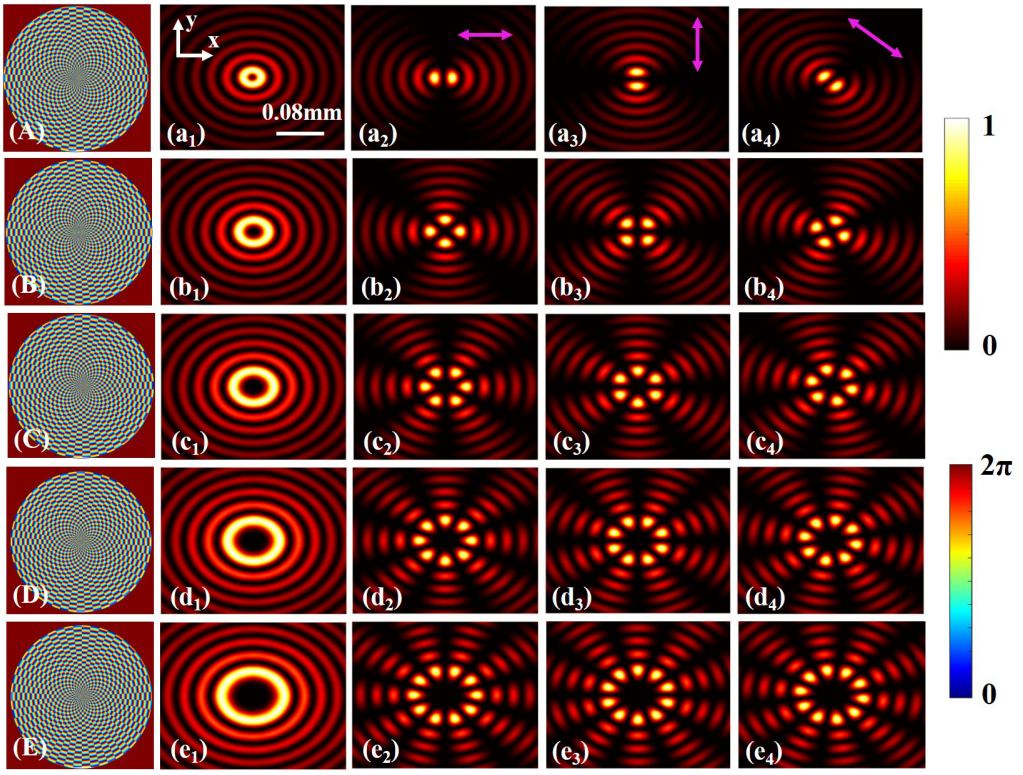

Fig. 3. Extraction results of different polarization modes of Bessel beam with topological number $l = 0$, where $\beta = 0$, $d = 0.07$. Polarization modes with the different order (a) $n = 1$, (b) $n = 2$, (c) $n = 3$, (d) $n = 4$, (e) $n = 5$ are extracted from $m = 30$-order vector vortex beam in the focal region based on the phases in (A)–(E), respectively. Subfigures (a_2)–(e_2), (a_3)–(e_3), (a_4)–(e_4) show the light intensities passing through the polarizer indicated by the pinkish purple arrows. The light intensities are normalized to a unit value, and the phase scale is 0–2π.

The extraction results of different polarization modes of Bessel beams with topological number $l = 0$ are demonstrated in Fig. 3. With regard to the vector Bessel beams, the order $n = 1, 2, 3, 4, 5$ are chosen. It can be seen that the central highlight ring of the total field keeps getting larger as the order n of the vector Bessel beam increases. Another characteristic of the vector Bessel beam is the polarization mode. The polarization vector changed with the rotation of the azimuth angle, and the number of petals is related to the order of the beam by $|2n|$.

The extraction results of different polarization modes of Bessel beams with topological number $l = 1$ are shown in Fig. 4. As the order n of the vector Bessel beams increases, the radius of the central dark zone of the total field becomes bigger except for Fig. 4(a_1), which are 0.008, 0.014, 0.024, and 0.034 mm. The center of the vector Bessel beam presents a solid bright spot in Fig. 4(a_1). Meanwhile, it is clear that there are two bright rings, and the intensity of the central bright ring is higher than that of the second bright ring (Fig. 4(b_1)–(e_1)). The double-ring petals are obtained when passing

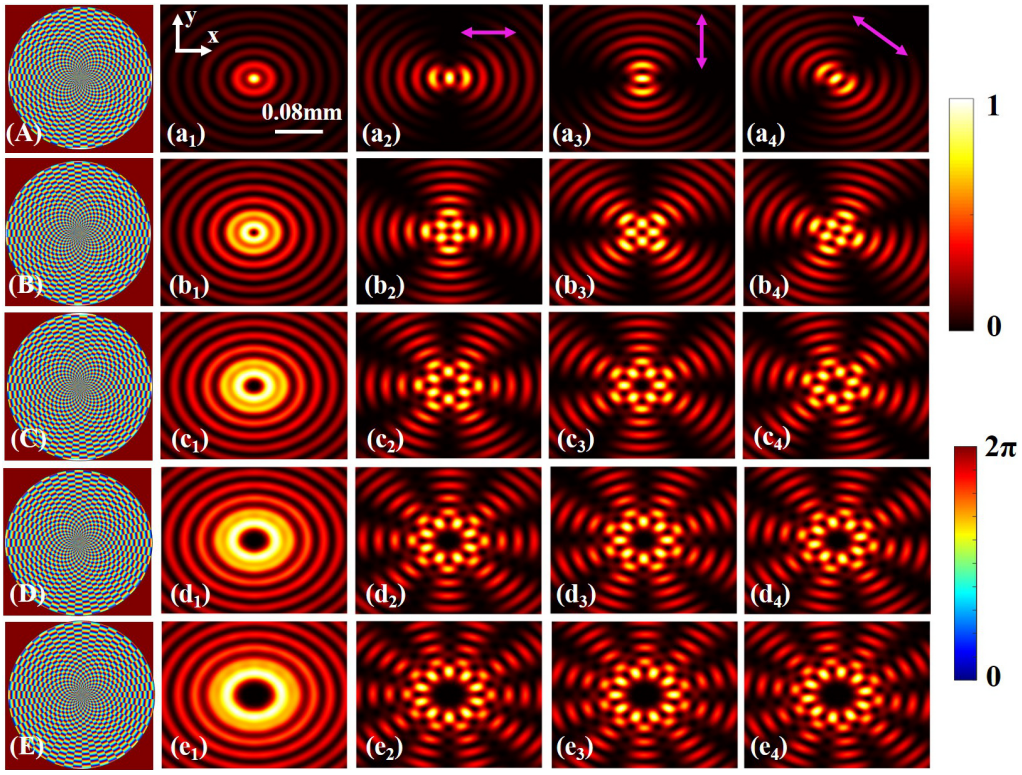

Fig. 4. Extraction results of different polarization modes of Bessel beam with topological number $l = 1$, where $\beta = 0$, $d = 0.07$. Polarization modes with the different order (a) $n = 1$, (b) $n = 2$, (c) $n = 3$, (d) $n = 4$, (e) $n = 5$ are extracted from $m = 30$-order vector vortex beam in the focal region based on the phases in (A)–(E), respectively. Subfigures (a_2)–(e_2), (a_3)–(e_3), (a_4)–(e_4) show the light intensities passing through the polarizer indicated by the pinkish purple arrows. The light intensities are normalized to a unit value, and the phase scale is 0–2π.

through the polarizer. And $|2n|$ petals are rotated with the polarizer indicated by the pink-purple arrows, as shown in Fig. 4(b_1)–(b_4), (c_1)–(c_4), (d_1)–(d_4), (e_1)–(e_4).

The extraction results of different polarization modes of Bessel beams with topological number $l = 2$ are depicted in Fig. 5. It can be seen that with the increase of the order n, the central dark area of the vector Bessel beams increases gradually except for Fig. 5(b_1)–(b_4). There are two inner rings with stronger light intensity, as shown in Fig. 5(a_1), (c_1), (d_1), (e_1). In addition, the total electric field distributions of the vector Bessel beams exhibit the central bright spot, and the light intensity is relatively weak when order $n = 2$, as shown in Fig. 5(b_1)–(b_4). Through the polarizer, the inner ring does not separate the petal, while the second ring separates $|2n|$ petals except for order $n = 1$. Notably, although the inner ring does not separate the petals, its light intensity is not uniformly distributed when order $n = 1$. Moreover, through the polarizer, the inner ring light intensities of the Fig. 5(a_2)–(a_4), (c_2)–(c_4) are stronger than that of the Fig. 5(d_2)–(d_4), (e_2)–(e_4).

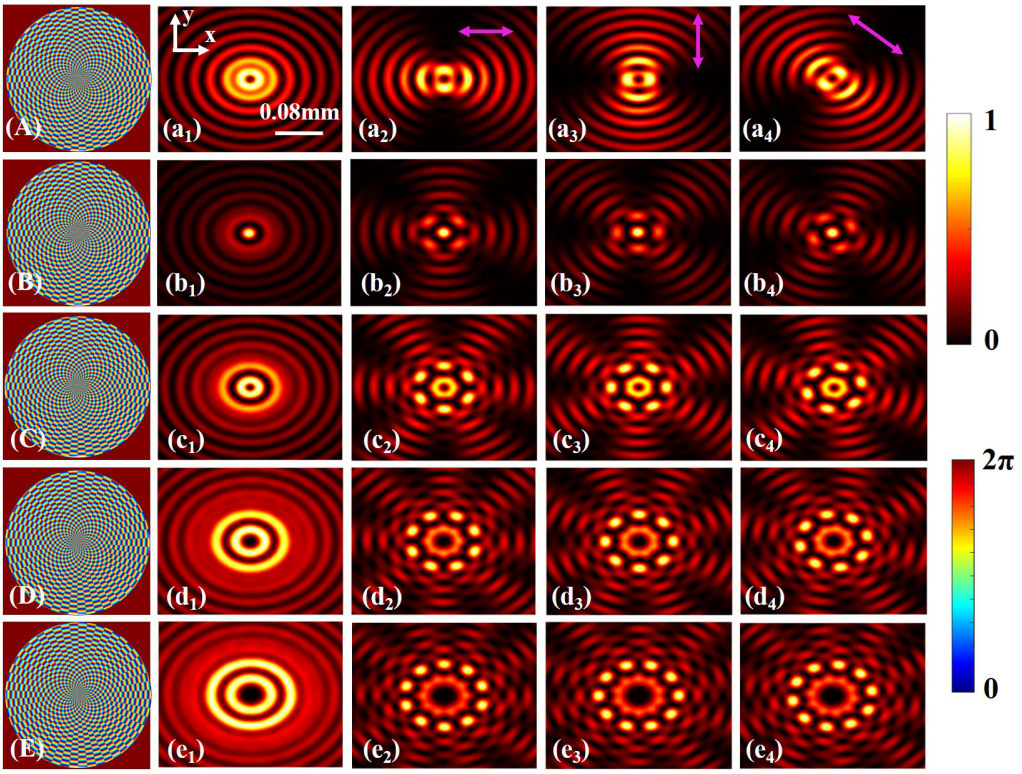

Fig. 5. Extraction results of different polarization modes of Bessel beam with topological number $l = 2$, where $\beta = 0$, $d = 0.07$. Polarization modes with the different order (a) $n = 1$, (b) $n = 2$, (c) $n = 3$, (d) $n = 4$, (e) $n = 5$ are extracted from $m = 30$-order vector vortex beam in the focal region based on the phases in (A)–(E), respectively. Subfigures (a_2)–(e_2), (a_3)–(e_3), (a_4)–(e_4) show the light intensities passing through the polarizer indicated by the pinkish purple arrows. The light intensities are normalized to a unit value, and the phase scale is 0–2π.

The polarization mode extraction results of vector Bessel beams with different topological numbers $l = 0, 1, 2$ are shown in Figs.3–5. Arbitrary polarization modes can be extracted from a single Bessel beam. Additionally, it is found that the vector Bessel beam shows the central bright spot when $n = l$. This can be attributed to the fact that the phase affects the polarization, and the phase singularity and the polarization singularity cancel each other out.

The polarization distributions of different order n where (a)–(e) respectively represent $n = 1, 2, 3, 4, 5$ are illustrated in Fig. 6. The polarization state is completely different with different order n. Therefore, arbitrary polarization modes can be extracted from the $m = 30$ order vortex wave plate. According to the theoretical analysis, the polarization distribution is independent from the topological number l of Bessel beam.

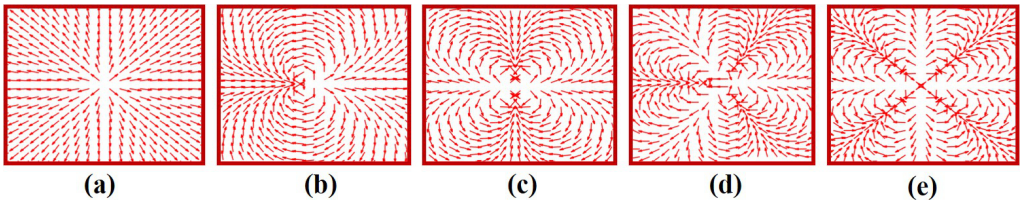

Fig. 6. The polarization distribution corresponding to different orders. (a) to (e) correspond to the order $n = 1, 2, 3, 4$, and 5, respectively.

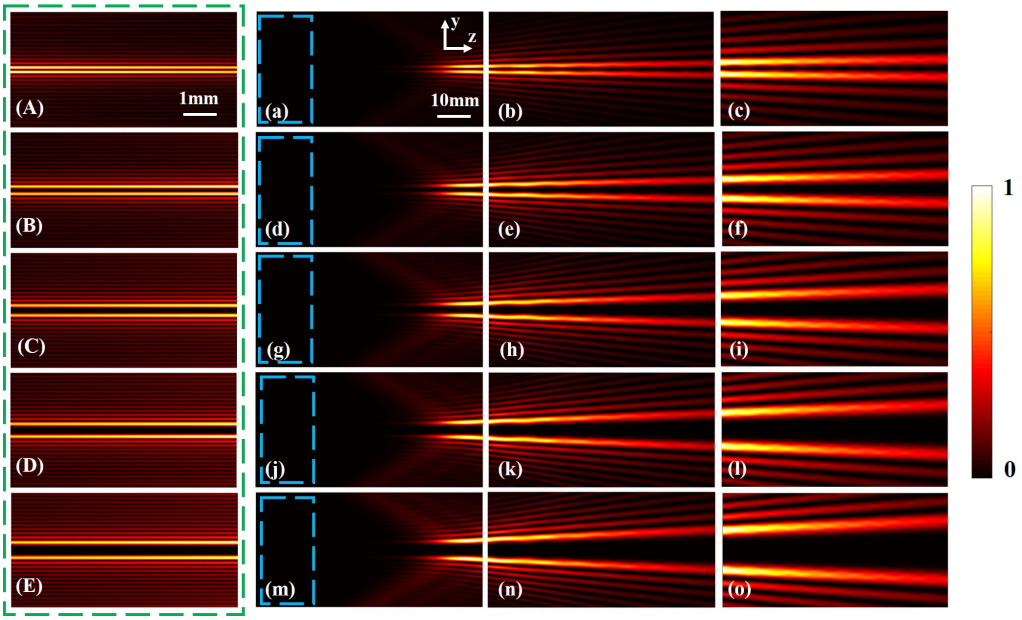

Fig. 7. Transmission field distribution of vector Bessel beam with topological number $l = 0$. (a)–(c) are $n = 1$. (d)–(f) are $n = 2$. (a)–(c) are $n = 3$. (g)–(i) are $n = 4$. (j)–(l) are $n = 5$. (m)–(o) are $n = 6$. (A)–(E) represent the transmission field distribution of the blue dashed box in (a), (d), (g), (j), (m). The light intensities are normalized to a unit value.

To further explore transmission properties of vector Bessel beam, we set $l = 0$, $\beta = 0$, and $n = 0, 1, 2, 3, 4, 5$ to observe their properties, as shown in Fig. 7. The field of view range of the second column is 0–100 mm, the third column is 100–200 mm, the fourth column is 200–300 mm. Where the green dashed box is part of the transmission field corresponding to the blue dashed box, as shown in Fig. 7(A)–(E). The blue dotted box is no light intensity, because of the normalization. It can be seen that the longitudinal distance of transmission field is wider with the order n increasing. The longitudinal distance is 0.01, 0.04, 0.056, 0.072, and 0.088 mm in Fig. 7(A)–(E), respectively. The transmission field distribution of vector Bessel beams has excellent directionality, collimation, and high brightness. However, as the distance increases, we find that the Bessel beam spreads, due to the diffractive properties.

In addition to extracting arbitrary polarization mode from a single Bessel beam, optical pen might be used to generate array of Bessel beams to achieve the extraction of multiple polarization modes. Here, as shown in Fig.8, the effect of polarization direction β and order n on polarization mode of vector Bessel beams is explored.

By means of the optical pen technology, the array of arbitrary modes can be generated by modulating the number and position of Bessel beam. The different patterns (*i.e.*, circles, squares and triangles) are designed in Fig. 8. Here, (a)–(c) change order

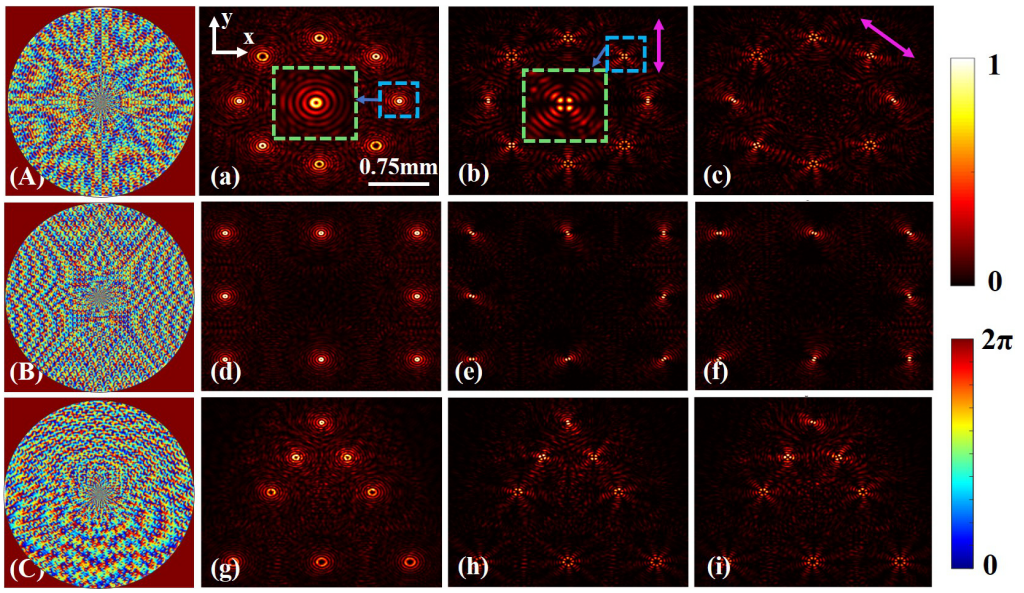

Fig. 8. Theoretical results of multiple polarization mode extraction. Different orders n are changed in (a)–(c) with $\beta = 0$. Different parameters β are changed in (d)–(f) with order $n = 1$. Both order n and parameter β are changed in (*g*)–(*i*). (a), (d), (g) are extracted from phase (A), (B), (C). Subfigures (b), (c), (e), (f), (h), and (i) show the light intensities passing through the polarizer indicated by the pinkish purple arrows. The spots in the green boxes in subfigures (a) and (b) are the magnified effect of the spots in the corresponding blue boxes. The light intensities are normalized to a unit value, and the phase scale is 0–2π.

$n = 1, 2, 3, 4$ to observe polarization mode, where $\beta = 0$, $l = 0$. (d)–(f) change parameter $\beta = 0, \pi/8, \pi/4, 3\pi/8, \pi/2, 5\pi/8, 7\pi/8$ to observe polarization mode, where $l = 0$, $n = 1$. (g)–(i) simultaneously vary the parameters β and n to observe the polarization mode, where $l = 0$. The first row of the triangle is $\beta = \pi/2$, and $n = 1$. The second row of the triangle is $\beta = 0, \pi/4$, and $n = 2$. The third row of the triangle is $\beta = 3\pi/8, 7\pi/8$, and $n = 3$. The fourth row of the triangle is $\beta = \pi/2, 3\pi/8, 5\pi/8$, and $n = 4$.

4. Experiment results and analysis

In order to verify the correctness of the arbitrary polarization mode extraction, an experimental setup for generating vector Bessel beam is designed as shown in Fig. 9. The incident beam is a laser with a wavelength of 780 nm, P was a polarizer, and the beam expanding collimation system is composed of lens L_1 ($f_1 = 50$ mm) and L_2 ($f_2 = 150$ mm). The phase only spatial light modulator (SLM) is entered through the beam splitter (BS), and the designed phase hologram is loaded into the SLM (HOLOEYE, model: PLUTO-2-NIR-011, pixel: 1920×1080, image element: 8.0 μm). L_3 ($f_3 = 100$ mm) and L_4 ($f_4 = 100$ mm) form a 4*f* system, which makes the phase encoding in SLM conjugate with the entrance plane of the 30-order vortex polarizer (VP). Finally, it is filtered by the 4*f* system, which consists of lens L_5 ($f_5 = 100$ mm) and L_6 ($f_6 = 100$ mm). Finally, the image is captured using a CCD (DAHENG IMAGING

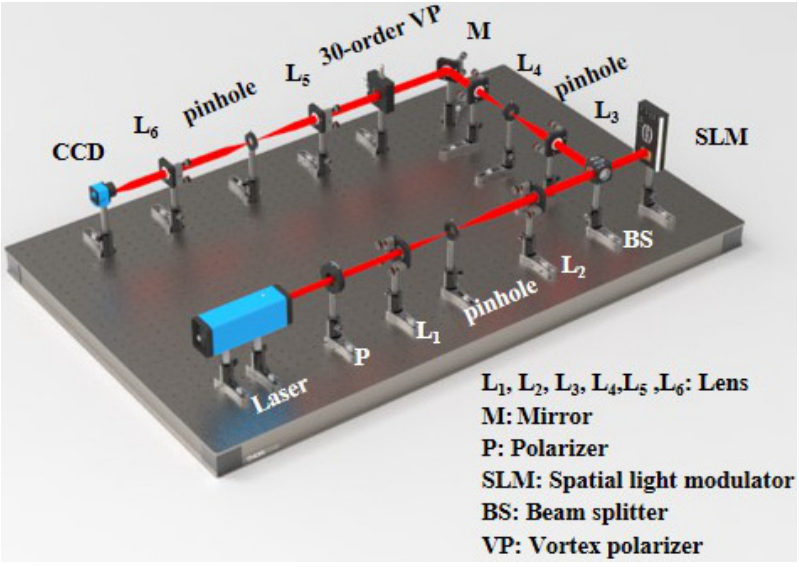

Fig. 9. Schematic diagram of experimental setup. The wavelength of the laser is 780 nm, P is the polarizer, M is the reflector, SLM is the reflective phase only spatial light modulator, L_1–L_6 are the lens ($f_1 = 50$ mm, $f_2 = 150$ mm, $f_3 = 100$ mm, $f_4 = 100$ mm, $f_5 = 100$ mm, $f_6 = 100$ mm). The calculated phase diagram is loaded into SLM, and CCD is used for image acquisition to record the focusing field distribution of vector Bessel beam under different orders.

MER-132-43U3C-L, pixel:1292 × 964, image element: 3.75 μm) to obtain the vector Bessel beam. The system could extract arbitrary polarization mode of vector Bessel beam.

The feasibility of the scheme is verified by calculating the phase hologram of the Bessel beam with the topological number $l = 0$. Loading phase order n respectively is 1, 2, 3, 4 and 5 to observe the light field distribution of Bessel beam collected by CCD. The obtained experimental results are shown in Fig. 10.

The experimental results generated by vector Bessel beam are described in Fig. 10. The orders n corresponding to (a)–(e) in the figure are 1, 2, 3, 4 and 5. (A)–(E) are the phase diagram of the corresponding Bessel beam. (a_1)–(e_1) are the total field intensity of the Bessel beam. The purple arrows indicate the direction of the polarizer at 0°, 90°, and 135°. By changing the direction of the polarizer, the different polarization distributions of the Bessel beam can be observed, as shown in Figs. (a_2)–(e_4). As can be observed in Fig. 10, $|2n|$ petals would be separated by changing the angle of the polarizer. The experiment proves the correctness of the above simulation results.

It is worth noting that the experimental results do not significantly recover to the 1:1 simulation results due to the possible existence of some aberrations in the setup.

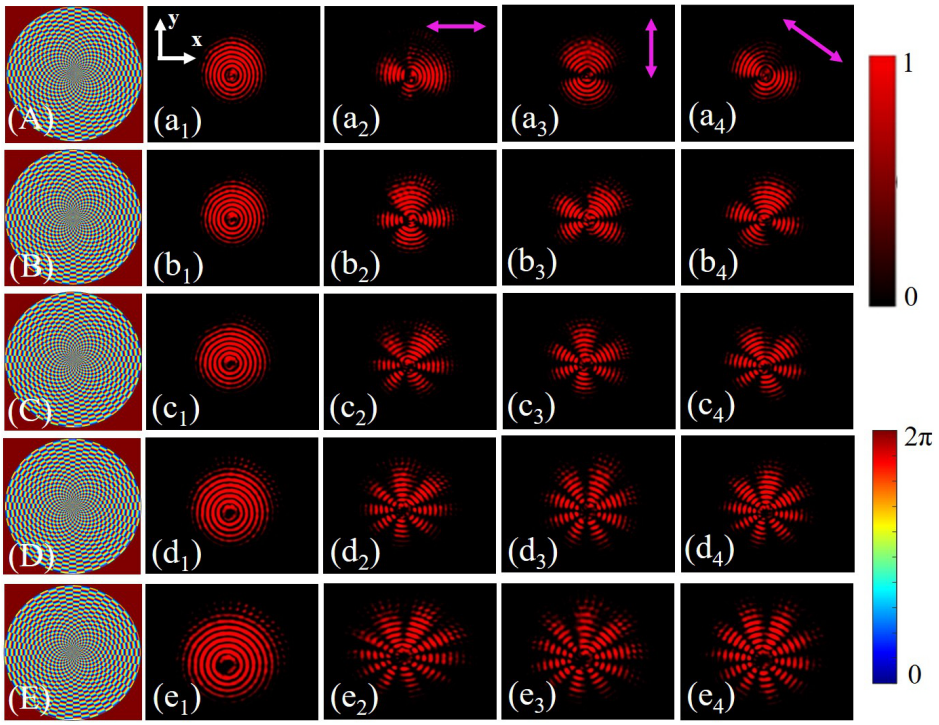

Fig. 10. Experimental results generated by vector Bessel beam. Here, (A)–(E) are Bessel phase diagrams of order $n = 1, 2, 3, 4, 5$, respectively. Subgraphs (a_1)-(e_1) are the total field distribution of Bessel beam. Graphs (a_2)–(e_2), (a_3)–(e_3), (a_4)–(e_4) are corresponding to polarizer of 0 °, 90 ° and 135 ° of the electric field distribution.

The purpose of this experiment is to verify the feasibility of the theoretical principle. We designed and built an experimental device to generate the vector Bessel beam, and confirmed that the system could extract any polarization mode of the vector Bessel beam, thus verifying the feasibility of the principle. Our research group will continue to carry out the next experiment based on this research in the later stage. We make full use of the optical pen technology and pattern extraction principle to explore more mechanisms and experiments on vector light field regulation, so as to enrich our subsequent research results.

5. Conclusion

In conclusion, we have verified the method of combining the mode extraction principle with the optical pen technique to create vector Bessel beams with arbitrary polarization mode in free space. Specifically, the omnidirectional modulation of the axicon parameters d, topology number l, order n, polarization direction β, as well as spatial position, quantity, *etc*. are achieved. This work has very important research significance and application value in many fields. Specifically, the vector Bezier beam polarization mode array generated in this paper can be used to improve the transmission rate of free-space optical communication through mode division multiplexing by using the spatially inhomogeneous states of polarization of vector modes. In addition, a vector beam that can freely adjust the degree of polarization and spatial freedom can provide more available states. It will provide more possibilities for applications such as optical communication, particle manipulation, super-resolution microscopic imaging, and quantum optics.

Acknowledgements
This work was supported by the National Key Research and Development Program of China (2018YFC1313803).

Disclosures
The authors declare no conflicts of interest.

Data availability
Data underlying the results presented in this paper are not publicly available at this time but may be obtained from the authors upon reasonable request.

References

[1] Durnin J., Miceli J.J., Eberly J.H., *Diffraction-free beams*, Physical Review Letters **58**(15), 1987: 1499-1501.
[2] Al-Awfi S., *Theory of evanescent Bessel beams with a metallic sheet*, Optica Applicata **43**(3), 2013: 539-550.
[3] Chen B.Y., Huang X.S., Gou D.Z., *Rapid volumetric imaging with Bessel-Beam three-photon microscopy*, Biomedical Optics Express **9**(4), 2018: 1992-2000.
[4] Drobczynski S., Dus-Szachniewicz K., Symonowicz K., *Spectral analysis by a video camera in a holographic optical tweezers setup*, Optica Applicata **43**(4), 2013: 739-746.

[5] BALTRUKONIS J., ULCINAS O., ORLOV O., *High-order vector Bessel-Gauss beams for laser micromachining of transparent materials*, Physical Review Applied **16**(3), 2021: 034001.
[6] RIOUX M., TREMBLAY R., BÉLANGER P.A., *Linear, annular, and radial focusing with axicons and applications to laser machining*, Applied Optics **17**(10), 1978: 1532-1536.
[7] ZHAO Y., SUN H., ZHANG X., WANG Y., *The interference characteristics of light-waves from a tilted and defocused cat-eye optical lens irradiated by laser beam*, Optica Applicata **41**(3), 2011: 617-630.
[8] ZHANG Y.X., DONG W.M., ZHANG Y., *All-fiber hollow Bessel-like beam for large-size particle trap*, Journal of Lightwave Technology **39**(10), 2021: 3291-3296.
[9] ZHANG Y.X., TANG X.Y., LIU Z.H., *Multiple particles 3-D trap based on all-fiber Bessel optical probe*, Journal of Lightwave Technology **35**(18), 2017: 3849-3853.
[10] GAO X., ZHANG D., MEI T., RUI F., ZHUANG S., *Focus shaping of the radially polarized Bessel-Gauss beam with a sine-azimuthal variation wavefront*, Optica Applicata **43**(3), 2013: 567-582.
[11] GAO X., GAO M., HU S., GUO H., ZHUANG S., *High focusing of radially polarized Bessel-modulated Gaussian beam*, Optica Applicata **40**(4), 2010: 965-974.
[12] YUAN Y.S., LEI T., LI Z.H., *Beam wander relieved orbital angular momentum communication in turbulent atmosphere using Bessel beams*, Scientific Reports **7**, 2017: 42276.
[13] OUBEI H.M., DURAN J.R., JANJUA B., *48 Gbit/s 16-QAM-OFDM transmission based on compact 450-nm laser for underwater wireless optical communication*, Optics Express **23**(18), 2015: 23302 -23309.
[14] WANG G., LI Y., SHAN X., MIAO Y., GAO X., *Hermite–Gaussian beams with sinusoidal vortex phase modulation*, Chinese Optics Letters **18**(4), 2020: 80-84.
[15] BANDO K., YABUUCHI S., LI M.L., *Bessel-beam illumination Raman microscopy*, Biomedical Optics Express **13**(6), 2022: 3161-3170.
[16] SHI H.T., SHEN G.Y., QI H.Y., *Noise-tolerant Bessel-beam single-photon imaging in fog*, Optics Express **30**(7), 2022: 12061-12068.
[17] LU Z.H., GUO Z.F., FAN M.S., *Tunable Bessel beam shaping for robust atmospheric optical communication*, Journal of Lightwave Technology **40**(15), 2022: 5097-5106.
[18] GUO L., TANG Z., *Vectorial structure and beam quality of vector-vortex Bessel-Gauss beams in the far-field*, Chinese Optics Letters **10**(Suppl.), 2012: S12601.
[19] MILIONE G., LAVERY M.P.J., HUANG H., REN Y., XIE G., NGUYEN T.A., KARIMI E., MARRUCCI L., NOLAN D.A., ALFANO R.R., WILLNER A.E., *4 × 20 Gbit/s mode division multiplexing over free space using vector modes and a q-plate mode (de)multiplexer*, Optics Letters **40**, 2015: 1980.
[20] NDAGANO B., NAPE I., COX M.A., ROSALES-GUZMAN C., FORBES A., *Creation and detection of vector vortex modes for classical and quantum communication*, Journal of Lightwave Technology **36**, 2018: 292-301.
[21] DORN R., QUABIS S., LEUCHS G., *Sharper focus for a radially polarized light beam*, Physical Review Letters **91**, 2003: 233901.
[22] HANSEN S.G., *Source mask polarization optimization*, Journal of Micro/Nanolithography, MEMS, and MOEMS **10**, 2011: 1-10.
[23] WANG H., SHI L., LUKYANCHUK B., SHEPPARD C., CHONG C.T., *Creation of a needle of longitudinally polarized light in vacuum using binary optics*, Nature Photonics **2**, 2008: 501-505.
[24] BOOTH M.J., *Adaptive optical microscopy: the ongoing quest for a perfect image*, Light: Science & Applications **3**, 2014: e165.
[25] NDAGANO B., NAPE I., COX M.A., ROSALES-GUZMAN C., FORBES A., *Creation and detection of vector vortex modes for classical and quantum communication*, Journal of Lightwave Technology **36**, 2018: 292-301.
[26] COZZOLINO D., POLINO E., VALERI M., CARVACHO G., BACCO D., SPAGNOLO N., OXENLØWE L.K., SCIARRINO F., *Air-core fiber distribution of hybrid vector vortex-polarization entangled states*, Advanced Photonics **1**, 2019: 1.
[27] FICKLER R., LAPKIEWICZ R., PLICK W.N., KRENN M., SCHAEFF C., RAMELOW S., ZEILINGER A., *Quantum entanglement of high angular momenta*, Science **338**, 2012: 640-643.

[28] Rao A.S., Samanta G.K., *On-axis intensity modulation-free, segmented, zero-order Bessel beams with tunable ranges*, Optics Letters **43**(13), 2018: 3029-3032.
[29] Niv A., Biener G., Kleiner V., *Propagation-invariant vectorial Bessel beams obtained by use of quantized Pancharatnam-Berry phase optical elements*, Optics Letters **29**(3), 2004: 238-240.
[30] Yang J.Q., Hakala T.K., Friberg A.T., *Generation of arbitrary vector Bessel beams on higher-order Poincaré spheres with an all-dielectric metasurface*, Physical Review A **106**(2), 2022: 023520.
[31] Li P., Zhang Y., Liu S., *Quasi-Bessel beams with longitudinally varying polarization state generated by employing spectrum engineering*, Optics Letters **41**(20), 2016: 4811-4814.
[32] Lin Z.M., Li X.W., Zhao R.Z., *High-efficiency Bessel beam array generation by Huygens metasurfaces*, Nanophotonics **8**(6), 2019: 1079-1085.
[33] Weng X.Y., Miao Y., Zhang Q.L., *Extraction of inherent polarization modes from a single light beam*, 2021. https://arxiv.org/abs/2102.11620v1
[34] Weng X., Song Q., Li X., Gao X., Guo H., Qu J., Zhuang S., *Free-space creation of ultralong anti -diffracting beam with multiple energy oscillations adjusted using optical pen*, Nature Communications **9**, 2018: 5035.
[35] Richards B., Wolf E., *Electromagnetic diffraction in optical systems. III. Structure of the image field in an aplanatic system*, Proceedings of the Royal Society A **253**, 1959: 358-379.
[36] Wang G.X., Kang X.Y., Sun X.J., *Generation of arbitrary perfect optical vortex in free space by optical pen*, Optics Express **30**(18), 2022: 31959-31970.
[37] Milione G., Lavery M.P.J., Huang H., Ren Y., Xie G., Nguyen T.A., Karimi E., Marrucci L., Nolan D.A., Alfano R.R., Willner A.E., *4×20 Gbit/s mode division multiplexing over free space using vector modes and a q-plate mode(de) multiplexer*, Optics Letters **40**, 2015: 1980-1983.
[38] Marrucci L., Manzo C., Paparo D., *Optical spin-to-orbital angular momentum conversion in inhomogeneous anisotropic media*, Physical Review Letters **96**(16), 2006: 163905.
[39] Gao C., Fu S., *Vortex Beams*, Tsinghua University Press, Beijing, 2019: 288-289 (in Chinese).

Received January 10, 2023
in revised form February 12, 2023